Mannodendrimers prevent acute lung inflammation by inhibiting neutrophil recruitment

Emilyne Blattes[a,b], Alain Vercellone[a,b], Hélène Eutamène[c,d], Cédric-Olivier Turrin[e,f], Vassilia Théodorou[c,d], Jean-Pierre Majoral[e,f], Anne-Marie Caminade[e,f], Jacques Prandi[a,b], Jérôme Nigou[a,b], and Germain Puzo[a,b,1]

[a]Centre National de la Recherche Scientifique, Institut de Pharmacologie et de Biologie Structurale, F-31077 Toulouse, France; [b]Université de Toulouse, Université Paul Sabatier, Institut de Pharmacologie et de Biologie Structurale, F-31077 Toulouse, France; [c]Institut National de la Recherche Agronomique, Toxicologie Alimentaire, F-31027 Toulouse, France; [d]Université de Toulouse, Université Paul Sabatier, Institut National Polytechnique de Toulouse, Toxicologie Alimentaire, F-31027 Toulouse, France; [e]Centre National de la Recherche Scientifique, Laboratoire de Chimie de Coordination, F-31077 Toulouse, France; [f]Université de Toulouse, Université Paul Sabatier, Institut National Polytechnique de Toulouse, Laboratoire de Chimie de Coordination, F-31077 Toulouse, France

Edited by Jerrold Meinwald, Cornell University, Ithaca, NY, and approved April 15, 2013 (received for review December 13, 2012)

Mycobacterium tuberculosis **mannose-capped lipoarabinomannan inhibits the release of proinflammatory cytokines by LPS-stimulated human dendritic cells (DCs) via targeting the C-type lectin receptor DC-specific intercellular adhesion molecule 3-grabbing nonintegrin (DC-SIGN). With the aim of mimicking the bioactive supramolecular structure of mannose-capped lipoarabinomannan, we designed and synthesized a set of poly(phosphorhydrazone) dendrimers grafted with mannose units, called mannodendrimers, that differed by size and the number and length of their (α1→2)-oligommanoside caps. A third-generation dendrimer bearing 48 trimannoside caps (3T) and a fourth-generation dendrimer bearing 96 dimannosides (4D) displayed the highest binding avidity for DC-SIGN. Moreover, these dendrimers inhibited proinflammatory cytokines, including TNF-α, production by LPS-stimulated DCs in a DC-SIGN–dependent fashion. Finally, in a model of acute lung inflammation in which mice were exposed to aerosolized LPS, *per os* administration of 3T mannodendrimer was found to significantly reduce neutrophil influx via targeting the DC-SIGN murine homolog SIGN-related 1. The 3T mannodendrimer therefore represents an innovative fully synthetic compound for the treatment of lung inflammatory diseases.**

antiinflammatory molecule | SIGNR1 targeting | glycodendrimer synthesis | multivalent ligands | ManLAM functional analogs

To secure their colonization and survival, some bacterial intracellular pathogens have evolved tactics to undermine host innate immune responses, including inflammation. *Mycobacterium tuberculosis*, the causative agent of human tuberculosis, uses multiple mechanisms to survive within its host cellular niches of alveolar macrophages and dendritic cells (DCs). In particular, *M. tuberculosis* exposes surface lipoglycans at its cell envelope, namely mannose-capped lipoarabinomannans (ManLAMs), which inhibit the production of proinflammatory cytokines IL-12 and TNF-α by LPS-stimulated human DCs (1–3) via binding to the C-type lectin DC-specific intercellular adhesion molecule 3 (ICAM-3)-grabbing nonintegrin (DC-SIGN) (4, 5). DC-SIGN reportedly modulates immune responses to several other pathogens, supporting its important role as an immunomodulatory receptor (6). ManLAMs are complex amphipathic macromolecules with an average molecular weight of 17 kDa that are composed of three domains: (*i*) a mannosyl-phosphatidyl-*myo*-inositol (MPI) anchor; (*ii*) a heteropolysaccharidic core composed of D-mannan and D-arabinan; and (*iii*) mannose caps consisting of mono, (α1→2)-di-, and (α1→2)-trimannosides (7). MPI anchor fatty acyl appendages induce a supramolecular organization of ManLAMs in aqueous solution, resulting in the formation of a 30-nm spherical structure of ∼450 molecules with the mannose caps exposed at the surface (8). This multivalent supramolecular structure allows multipoint attachment of ManLAMs, via mannose caps, to multimeric DC-SIGN receptors (9, 10) expressed at the surface of DCs, thereby ensuring high-affinity binding to the receptor (8–10) and induction of antiinflammatory activity (1, 2, 7).

The strategy used by *M. tuberculosis* to down-regulate the host inflammatory response prompted us to design synthetic molecules that mimic the bioactive supramolecular structure of ManLAMs, with the objective of developing innovative antiinflammatory molecules. The task required development of a spherical backbone or scaffold, and then functionalization of this scaffold by linear mannooligosaccharide caps. Dendrimers are compounds of choice to generate 3D structures (11). They are monodisperse, polyfunctionalized, and hyperbranched macromolecules whose nanometer size, multivalent character, and molecular weight can be controlled rigorously during synthesis (11). Dendrimers can adopt a spherical conformation and are particularly amenable to surface attachment of multiple copies of ligands closely packed, leading to a high density of ligands and, consequently, to synthetic molecules with a higher valency and avidity for C-type lectins (9).

Here, we report the synthesis, using the poly(phosphorhydrazone) (PPH) scaffold (11, 12), of a family of mannosylated dendrimers (hereafter referred to as mannodendrimers) differing by the number of generations and the structure of mannose caps. The third-generation mannodendrimer capped with (α1→2)-trimannopyranosides (3T) was a powerful antiinflammatory compound that reduced lung accumulation of neutrophils in a mouse model of acute lung inflammation.

Results

Synthesis of Mannose-Capped PPH Dendrimers. Mannosylated PPH dendrimers were synthesized by grafting synthetic mono, (α1→2)-di-, or (α1→2)-trimannopyranosides (M, D, and T, respectively; Fig. S1*A*) found in ManLAM caps to the surface of dendrimers. The D and T structures were synthesized by successive additions of D-mannose units to a suitable linker using standard glycosylation conditions that allowed full control of the α-configuration of the anomeric centers (13). Once this process was complete, (α1→2)-oligomannosides were fully deprotected before coupling with the PPH dendrimers. A short 3-hydroxypropionic acid linker was used for elaboration of the dendrimers from the first to the third generations substituted by α-D-mannopyranosides. For all other mannodendrimers, the longer 9-hydroxynonanoic acid linker was used (Fig. S1*A*) to allow greater flexibility of the (1→2)-oligomannosides and to overcome the steric crowding at the surface of the dendrimer.

The acyl-azide coupling method (14) was used to link alkyl-oligomannosides to the dendrimer surface; this method required

Author contributions: E.B., A.V., H.E., C.-O.T., V.T., J.-P.M., A.-M.C., J.P., J.N., and G.P. designed research; E.B., A.V., and H.E. performed research; E.B., A.V., H.E., C.-O.T., V.T., J.-P.M., A.-M.C., J.P., J.N., and G.P. analyzed data; and E.B., J.N., and G.P. wrote the paper.

The authors declare no conflict of interest.

This article is a PNAS Direct Submission.

[1]To whom correspondence should be addressed. E-mail: Germain.Puzo@ipbs.fr.

This article contains supporting information online at www.pnas.org/lookup/suppl/doi:10.1073/pnas.1221708110/-/DCSupplemental.

preparation of PPH dendrimers with an NH_2-derivatized surface (12) that were obtained by reaction of the growing dendrimer [generations 1–4 with $P(S)Cl_2$ surface] with the alcohol function of *N-tert*-butoxycarbonyl tyramine (N-BOC tyramine). The reaction time for this substitution was highly dependent on generation of the dendrimer; the progress of the reaction was monitored by ^{31}P NMR spectroscopy of the crude reaction mixture (Fig. S1*B*, reaction 1). Monosubstitution of each phosphorus end group was first observed as the appearance of a singlet at 68.5 ppm on the ^{31}P NMR spectrum, and this structure evolved to a disubstituted hydrazidothiophosphate (singlet at 63 ppm). For the four generations of PPH dendrimers analyzed by ^{31}P NMR, the resonance of phosphorus atoms of the core and branches showed similar chemical shifts at 8.5 and ∼62.5 ppm, respectively. Deprotection of the BOC group under acidic conditions produced the required dendrimers with NH_3^+ groups on their surface, as indicated by the disappearance of the BOC signal on the ^1H NMR spectra (Figs. S1*B*, reaction 2, and S2*A*). The (α1→2)-oligomannosides were activated into acyl azides and coupled to the dendrimers (Fig. S1*B*, reactions 3, 4, and 5). High amounts of triethylamine (pH ≥ 9) were added to the reaction mixture to deprotonate dendrimers and to allow end-group substitution; this process was monitored by ^1H and ^{31}P NMR. Performing the coupling reaction three or four times with an excess of (α1→2)-oligomannosides was necessary to achieve complete substitution. The mannodendrimers were then purified by size-exclusion chromatography in endotoxin-free water and were fully characterized by ^1H (Fig. S2*A*), ^{13}C, and ^{31}P NMR spectroscopy. Covalent connection between the oligomannoside linker and the mannodendrimer skeleton was firmly established from the ^1H-^{13}C HMBC correlation spectrum showing a scalar coupling of the carbonyl group of the linker with the aminomethylene protons of the dendrimer (Fig. S2*A*). The eight mannodendrimers (1M, 2M, 3M, 1D, 2D, 3D, 3T, and 4D) (Table 1) were obtained at a good yield (∼30%), at the dozens of milligrams scale. Fig. S2*C* shows the full NMR characterization of 3T mannodendrimer, whereas Fig. 1*A* represents its partial structure in which only one of the six branches around the core is displayed.

Binding of Mannodendrimers to DC-SIGN. Mannodendrimers were first evaluated for their ability to bind to the human DC-SIGN receptor. An inhibition binding assay using a recombinant soluble tetrameric form of the DC-SIGN protein (sDC-SIGN) and ManLAM-coated microplates was developed (Fig. S3 *A* and *B*). All of the mannodendrimers synthesized were able to bind sDC-SIGN (Fig. S3*E*). Interestingly, the 3M, 3D, 3T, and 4D mannodendrimers displayed a binding efficiency similar to that of *M. tuberculosis* ManLAM. Taken together, these data indicated that efficient binding to sDC-SIGN requires at least a third-generation mannodendrimer, regardless of the cap length.

We further examined the binding of mannodendrimers to the full-length cell membrane-expressed DC-SIGN receptor (mDC-SIGN), using stably transfected HEK293 cells expressing the wild-type DC-SIGN protein N-terminally fused with the green fluorescent protein (GFP) (HEK::DC-SIGN) (Fig. S3*C*). Mannodendrimers were tested for their capacity to inhibit mDC-SIGN–dependent binding of HEK::DC-SIGN cells to mannan-coated microplates (Fig. S3*D*). IC_{50} values were determined for all mannodendrimers, with the exception of 1M, which was poorly inhibitory with an estimated IC_{50} value greater than 1 mM. As observed for the sDC-SIGN receptor, the effect of the mannodendrimer scaffold size was critical to its inhibitory activity toward binding of mDC-SIGN and IC_{50} values were proportional to the dendrimer generation (Fig. 1*B*). For instance, for dimannoside-capped dendrimers, the IC_{50} values decreased from 490 ± 170 nM for 1D to 166 ± 88 and 3.0 ± 0.5 nM for 2D and 3D, respectively. In contrast to the data obtained with sDC-SIGN, the cap length was determinant for binding of the third-generation mannodendrimers to mDC-SIGN; the IC_{50} value decreased from 1.1 ± 0.3 μM for 3M to 3 ± 0.5 and 5 ± 2 nM for 3D and 3T, respectively.

Interestingly, 3D, 4D, and 3T had IC_{50} values of ∼5 nM. This value is similar to that of ManLAM particle (ManLAM*) (Fig. 1*B*), which is the bioactive form of ManLAM composed of ∼450 ManLAM monomers (8) and with an average molecular weight of 7.6×10^6 g/mol.

Mannodendrimers Selectively Bind DC-SIGN on Human DCs. Human DCs express different C-type lectins at their surface, including DC-SIGN and mannose receptor (MR), both of which were previously reported to bind ManLAMs (4, 5, 15, 16). Among 3D, 4D, and 3T mannodendrimers that showed similar IC_{50} values, we selected one dendrimer of each generation, 3T and 4D, to synthesize fluorescent derivatives (3TF and 4DF, respectively), via a 10% statistical labeling of the $P(S)Cl_2$ dendrimer groups with conjugated julolidine before oligomannoside substitution (Fig. 2*A*) (17). 3TF and 4DF showed the same IC_{50} values toward sDC-SIGN as their unlabeled counterparts, indicating that grafting of the fluorescent dye had not affected mannodendrimer binding. Moreover, flow cytometry analyses revealed that 3TF (Fig. 2*B*) and 4DF (Fig. S4*A*) directly interacted with mDC-SIGN on HEK::DC-SIGN cells as efficiently as fluorescein hydrazide-labeled ManLAM (ManLAMF) (3, 15). In addition, 3TF (Fig. 2*B*) and 4DF (Fig. S4*B*) bound efficiently to human MR expressed on Rat6 cells, indicating that, like ManLAM (15, 16), 3T and 4D mannodendrimers are also ligands of the human MR.

Like ManLAMF, the 3TF (Fig. 2*C*) and 4DF (Fig. S4*D*) mannodendrimers efficiently bound DCs. The interaction was partially inhibited by an anti–DC-SIGN antibody, but not by anti-MR antibody (Fig. 2*D* and Fig. S4*D*). However, anti-MR antibody was able to inhibit 3TF binding to human MR expressed on Rat6 cells (Fig. S4*C*). Altogether, the data revealed that 3T and 4D mannodendrimers selectively bind DC-SIGN on DCs, as previously reported for ManLAM (4).

Mannodendrimers 3T and 4D Inhibit TNF-α Production by LPS-Stimulated DCs in a DC-SIGN–Dependent Fashion. Given that 3T and 4D mannodendrimers targeted DC-SIGN on DCs, we tested the capacity of these molecules to inhibit production of proinflammatory cytokines by LPS-stimulated DCs. In the absence of LPS, 3T and 4D mannodendrimers at a concentration of 0.6 μM had no effect on TNF-α production (Fig. 3*A*). By contrast, when DCs were stimulated by LPS, both mannodendrimers inhibited

Table 1. Structural features of synthesized mannodendrimers

	Name							
Feature	1M	2M	3M	1D	2D	3D	4D	3T
Generation	1	2	3	1	2	3	4	3
No. of caps	12	24	48	12	24	48	96	48
Mannoside	Mono	Mono	Mono	Di	Di	Di	Di	Tri
MW, g·mol^{-1}	5,846.7	12,825.7	26,639.3	8,658.1	18,448.6	37,993.4	76,999.1	48,118.2

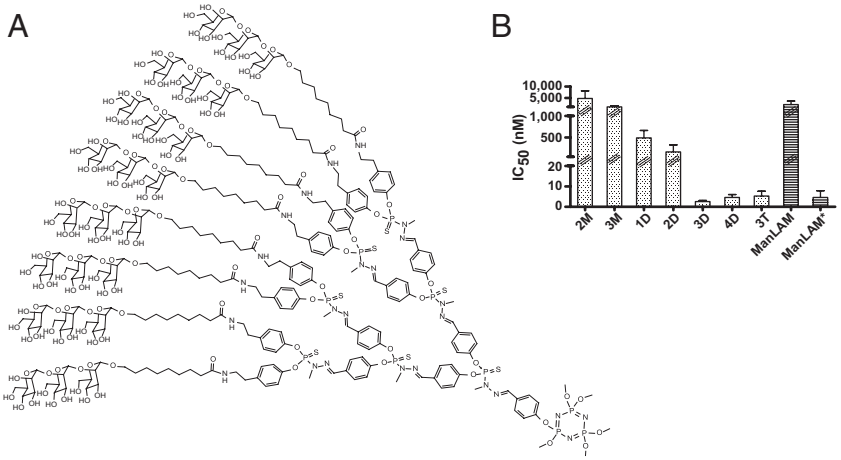

Fig. 1. Partial structure of mannodendrimer 3T (*A*) and binding of mannodendrimers to membrane-expressed DC-SIGN (*B*). (*A*) The 3T structure corresponds to a third-generation PPH dendrimer capped with (α1→2)-trimannopyranosides. One of the six branches around the core is shown. (*B*) IC_{50} values determined from the inhibition curves of HEK::DC-SIGN cells binding to mannan-coated plates. Inhibition curves with $R^2 \geq 0.90$ from four independent experiments were used to generate the IC_{50} values.

TNF-α production in a dose-dependent fashion; at a concentration of 0.6 μM, 3T and 4D reduced TNF-α production by 55% and 43%, respectively (Fig. 3*A*). Although, in our DC-SIGN binding assay, 3D exhibited an IC_{50} value similar to that of 3T and 4D, this molecule failed to inhibit TNF-α production (Fig. S5*A*). As expected, 2D, which interacts weakly with mDC-SIGN (Fig. 1*B*), also showed no inhibitory activity (Fig. 3*A* and Fig. S5*A*). The antiinflammatory activity of 3T (Fig. 3*B*) and 4D (Fig. S5*B*) mannodendrimers was completely abolished when DCs were preincubated with the anti–DC-SIGN AZND1 antagonist antibody (4), demonstrating that the activity was mediated by DC-SIGN.

As observed for TNF-α, 3T mannodendrimer was able to dose-dependently reduce the production of IL-6 and IL-8 by LPS-stimulated DCs (Fig. 3*C*). Interestingly, it increased the production of the antiinflammatory cytokine IL-10 (Fig. 3*C*) as previously described for ManLAM (4).

The signaling pathway involved was next investigated. DC-SIGN triggering on human DCs was previously found to activate the phosphorylation on two sites (Ser-338 and Tyr-340/341) of the serine and threonine kinase Raf-1, which, upon activation of Toll-like receptor 4 (TLR4) signaling, subsequently leads to acetylation of the NF-κB subunit p65 (6). Flow cytometry analysis showed that 3T induced Raf-1 phosphorylation on Tyr340/Tyr341 after 10 min of stimulation with LPS (Fig. 3*D*). Raf-1 phosphorylation was strongly reduced when DCs were preincubated with the AZND1 anti–DC-SIGN antibody or with the Src kinase inhibitor PP2.

Altogether, these data indicate that the 3T mannodendrimer modulates LPS-induced TLR4 signaling in a DC-SIGN– and Raf-1–dependent manner.

Mannodendrimer 3T and ManLAM Inhibit Lung Neutrophil Recruitment in a Mouse Model of Acute Lung Inflammation. Because 3T and 4D mannodendrimers mimicked ManLAM antiinflammatory activity in vitro, we tested the effect of the more potent 3T molecule in a validated mouse model of acute lung inflammation, which involved exposure of mice to aerosolized LPS (Fig. 4*A*).

We first showed that 3T was able to reduce the production of TNF-α, and chemokine (C-X-C motif) ligand 1 (CXCL-1) and CXCL-2 chemokines, by LPS-stimulated murine DCs in vitro (Fig. S6*A*). Then, infiltration of neutrophils into the lungs, which

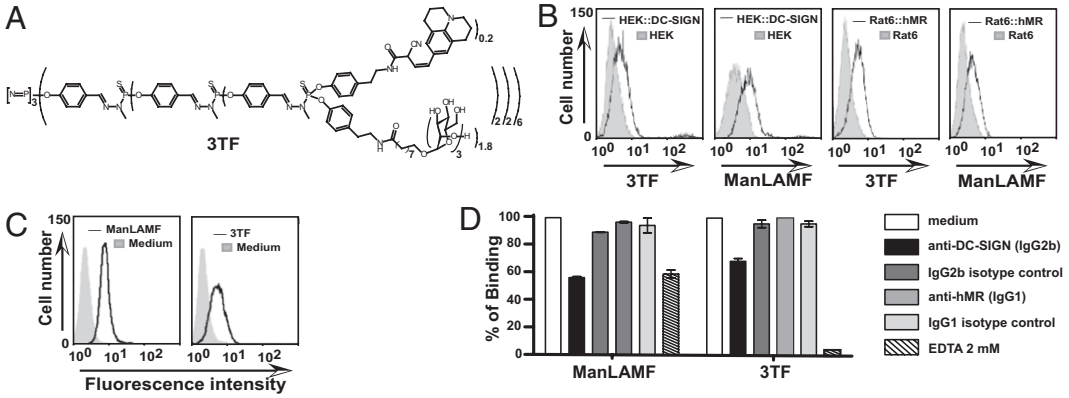

Fig. 2. The 3TF mannodendrimer selectively binds DC-SIGN on DCs. (*A*) Structure of the fluorescent 3TF dendrimer presenting up to 10% of julolidine at the surface. (*B*) Interaction of 3TF and ManLAMF with DC-SIGN and human MR (hMR) expressed in cell lines. One representative flow cytometry experiment (from three repeats) is shown for each cell line. (*C*) Binding of 3TF and ManLAMF to DCs. One representative flow cytometry experiment (from three repeats) is shown. (*D*) Binding of ManLAMF and 3TF to DCs is partially inhibited by preincubation of DCs with anti–DC-SIGN blocking antibody but not by anti-hMR blocking antibody (15 μg/mL). Data from flow cytometry analyses are expressed as a percentage of the control cells which were not preincubated with antibody (medium). Mean ± SD of three independent experiments are shown.

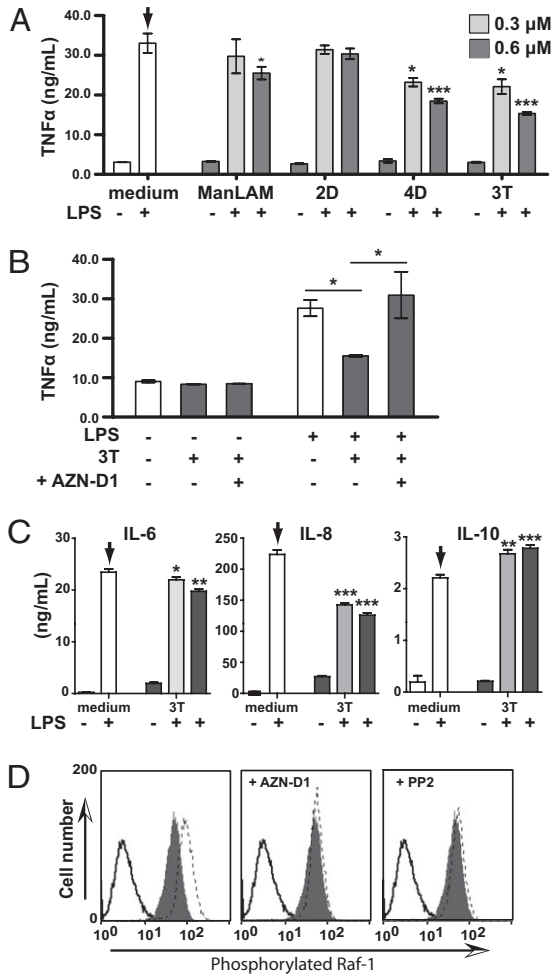

Fig. 3. Mannodendrimers 3T and 4D inhibit TNF-α production by LPS-stimulated human DCs. (*A*–*C*) DCs were stimulated by exposure to *E. coli* K12 LPS (20 ng/mL) in the presence or absence of 0.3 or 0.6 μM mannodendrimers or ManLAM. After 18 h, TNF-α, IL-6, IL-10, and/or IL-8 were measured in the culture supernatant. (*B*) The inhibitory activity of 3T (at 0.6 μM) on TNF-α release was abolished by preincubation of DCs with anti–DC-SIGN blocking antibody (AZND1; 20 μg/mL). One representative experiment (from three repeats) is shown. Data show mean ± SD. $*P < 0.05$, $***P < 0.001$. In *A* and *C*, statistical significance of the change in cytokine production was determined relative to LPS-exposed control cells (indicated by the bold arrow). (*D*) Raf-1 phosphorylation on Tyr340/Tyr341 in DCs in presence of LPS (20 ng/mL), 3T (0.6 μM), AZND1 (20 μg/mL), and Src Inhibitor PP2 (10 μM). Bold line, nonstimulated, not labeled DCs; filled line, nonstimulated DCs, labeled with anti-phosphorylated Raf-1; dotted line, LPS- and 3T-stimulated DCs, labeled with anti-phosphorylated Raf-1.

is an important component of the inflammatory response in acute lung injury, was monitored by quantifying neutrophils in the bronchoalveolar lavage fluids (BALFs). Exposure of C57BL/6 mice to LPS inhalation (1 mg) resulted in a dramatic recruitment of polymorphonuclear neutrophils to the lung that peaked at 18 h posttreatment. Mice were treated *per os* daily for 15 d with saline, 3T mannodendrimer, or ManLAM at a dose of 1 mg/kg, and then exposed (or not) to LPS inhalation (Fig. 4*A*). After 18 h, BALFs were collected and neutrophils were counted. In the absence of LPS inhalation, oral administration of 3T mannodendrimer or ManLAM did not induce neutrophil recruitment in the lungs (Fig. 4*B*). Interestingly, compared with the saline-fed mice, pretreatment with 3T or ManLAM significantly reduced the recruitment of neutrophils to the lungs in LPS-exposed mice by ~42% ($P < 0.001$) and 27% ($P < 0.001$), respectively. These data suggest that, in the model described here, *per os* administration of 3T mannodendrimer can prevent acute lung inflammation by significantly reducing neutrophil recruitment. The 3T mannodendrimer consistently showed a more potent in vivo antiinflammatory activity than ManLAM (Fig. 4*B*). Similar results were obtained with BALB/c mice (Fig. S7). 3T activity was further supported by histopathology analysis of the lungs (Fig. S8) and cytokine assay in BALF (Fig. S6*B*). Indeed, 3T prevented alveolar wall thickening and inflammatory cell infiltration (Fig. S8) and significantly reduced TNF-α release (Fig. S6*B*) observed in LPS-challenged mice. In contrast, 3T pretreatment had no impact on the production in lungs of IL-10 antiinflammatory cytokine or CXCL-1 and CXCL-2 chemokines (Fig. S6*B*).

Mice treated with 3T for 15 d were evaluated for their appearance and behavior (body weight, coat hair, gait, activity level, and posture), and macroscopic examinations of the spleen, liver, intestine, and lymph nodes were also performed. No differences were observed between 3T-treated and nontreated animals.

Murine DC-SIGN Homolog SIGN-Related 1 Mediates the in Vivo Antiinflammatory Activity of 3T Mannodendrimer and ManLAM. Experiments were performed to identify the mouse receptor responsible for mediating the in vivo antiinflammatory activity of both ManLAM and the 3T mannodendrimer. The mouse genome

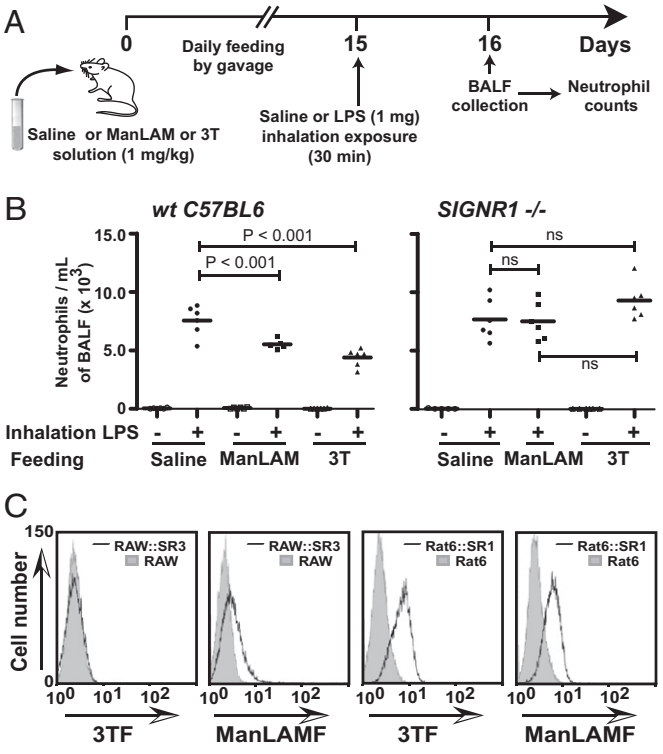

Fig. 4. Mannodendrimer 3T and ManLAM inhibit lung neutrophil recruitment in a mouse model of acute lung inflammation via the DC-SIGN murine homolog SIGNR1. (*A*) Mice treatment schedule; mice were fed daily with 3T mannodendrimer or ManLAM solution (1 mg/kg). At day 15, mice were aerosolized with LPS (1 mg) for 30 min. Eighteen hours later, mice were anesthetized using pentobarbital and the number of neutrophils per milliliter of bronchoalveolar lavage fluid (BALF) was determined. (*B*) Neutrophil recruitment in the lungs of LPS-aerosolized C57BL6 mice (wild type or SIGNR1 deficient), pretreated with either saline, 3T mannodendrimer, or ManLAM. Each geometric symbol represents one animal. Data are representative of at least two independent experiments. (*C*) Interaction of 3TF and ManLAMF with mouse receptors SIGNR1 (SR1) and SIGNR3 (SR3) expressed in RAW and Rat6 cell lines. One representative flow cytometry experiment (from three repeats) is shown for each cell line.

contains a DC-SIGN locus that encodes at least seven proteins, namely SIGN-related 1 (SIGNR1) to -5 and SIGNR7 to -8 (18). We have previously identified SIGNR1 and SIGNR3 as DC-SIGN homologs that interact with ManLAM (19); accordingly, flow cytometry analyses showed that ManLAMF bound both SIGNR3 expressed on RAW cells and SIGNR1 expressed on Rat6 cells (Fig. 4*C*). By contrast, the 3TF mannodendrimer bound SIGNR1 but not SIGNR3 (Fig. 4*C*). These results prompted us to test SIGNR1 as the candidate receptor mediating the in vivo antiinflammatory activity of 3T and ManLAM.

Both 3T and ManLAM were evaluated in the model of acute lung inflammation (Fig. 4*A*), using *Signr1*-deficient C57BL/6 mice (*Signr1*$^{-/-}$). Exposure of the latter to LPS resulted in a lung neutrophil recruitment similar to that observed in the wild-type C57BL/6 mice (Fig. 4*B*). However, pretreatment of the SIGNR1-deficient mice with ManLAM or 3T mannodendrimer failed to inhibit lung neutrophil recruitment in LPS-challenged animals. Mean concentrations of 7.6×10^3, 7.6×10^3, and 9.3×10^3 neutrophils per mL of BALF were observed in the groups of mice fed with saline, ManLAM, or 3T mannodendrimer, respectively (Fig. 4*B*). In summary, these findings indicate that the in vivo antiinflammatory activity of ManLAM and 3T mannodendrimer, which is characterized by a reduction of neutrophil recruitment in the lung of LPS-challenged mice, is dependent on the mouse DC-SIGN homolog SIGNR1.

Discussion

Glycodendrimers bearing covalently bound α-D-mannopyrannoside were previously synthesized from commercially available dendrimers, poly(L-lysine) (20) and poly(amidoamine) (21) scaffolds. PPH dendrimers, variously functionalized at their surface, have been shown to display numerous biological properties (11, 22) but have not yet been used for the grafting of mannose moieties. To mimic the antiinflammatory bioactive supramolecular structure of ManLAM (1, 8), we designed and optimized synthesis of a family of mannodendrimers based on the PPH scaffold. The synthesis was oriented toward the most active molecules, as identified by a series of bioassays, including binding avidity to the DC-SIGN receptor and inhibition of proinflammatory cytokine production by LPS-stimulated DCs. Initially, we found that all mannodendrimers bound to sDC-SIGN, but the dendrimers of the third generation and beyond that were capped with mono-, di-, or trimannoside caps were the best ligands of sDC-SIGN. The mannodendrimer structural requirements for binding to membrane-expressed DC-SIGN remained mostly the same, with the exception that the mannose cap length also became a critical parameter for binding. Interestingly, third-generation mannodendrimers carrying (α1→2)-di- (3D) or trimannoside (3T) units (with 48 caps) bound to membrane-expressed DC-SIGN as efficiently as the ManLAM bioactive particle. The effect of the molecular size was previously reported for other glycodendrimers targeting DC-SIGN (23). The higher avidity of dimannoside- and trimannoside-capped dendrimers versus single-mannose capped "ones" is in agreement with the crystal structure of the DC-SIGN carbohydrate recognition domain (CRD) in complex with an oligomannoside showing that this domain preferentially binds internal rather than terminal mannosyl residues (9, 10). In addition, DC-SIGN is a transmembrane protein that is organized as tetramers (9) and distributed as clustered patches at the cell surface (24). Therefore, the high functionalization of third-generation dendrimers with 48 mannosylated caps led to efficient multipoint attachment to the receptor; this degree of attachment seems optimum because avidity was not improved by a fourth-generation scaffold.

Like ManLAM (4), 3T and 4D mannodendrimers were found to selectively bind DC-SIGN on DCs. Although MR is able to bind mannodendrimers and ManLAM when it is individually expressed on Rat6 cells, the receptor does not participate in recognition of these molecules when it is coexpressed with DC-SIGN at the surface of DCs. The selectivity for DC-SIGN on DCs might be explained by two different properties of this receptor that are not shared by the MR: (*i*) DC-SIGN CRDs spike up from the cell surface (320 Å) (25) and might be encountered first, and (*ii*) DC-SIGN is distributed as clusters of tetramers (9, 24) that might constitute a platform of high avidity for mannodendrimers and ManLAM.

We found that submicromolar concentrations of 3T and 4D, but not 2D or 3D, inhibited TLR4-mediated TNF-α production by LPS-stimulated DCs in a DC-SIGN–dependent manner. These findings correlated with the high IC_{50} value of 2D (166 ± 88 nM), compared with the relatively lower IC_{50} value of 3T and 4D (5 ± 2 nM), but did not correlate with the similar IC_{50} value of 3D (3 ± 0.5 nM). Our findings suggest that the mannodendrimer IC_{50} values were therefore not completely sufficient for prediction of their capacity to inhibit production of proinflammatory cytokines in a DC-SIGN–dependent fashion. Signaling via DC-SIGN required a dendrimer scaffold size of third generation or fourth generation, substituted by trimannosides and dimannosides, respectively.

Finally, 3T mannodendrimer antiinflammatory activity was extended to inhibition of other inflammatory cytokine or chemokine, such as IL-6 and IL-8, and to stimulation of antiinflammatory cytokine IL-10, as previously observed for ManLAM (4).

Polyvalent dendrimer glucosamine conjugates were previously reported to prevent scar tissue formation in a rabbit model, thanks to antiangiogenic properties, and by inhibiting TLR4-mediated LPS-induced production of proinflammatory cytokines and chemokines by DCs (26). TLR4 plays a critical role in the pathogenesis of inflammation and is a key receptor involved in the LPS-induced neutrophil accumulation into lungs that underlies pulmonary failure leading to sepsis-related death (27). Neutrophil sequestration into the lungs and associated inflammatory damage is believed to contribute to the pathogenesis of diverse lung diseases, including acute lung injury and the acute respiratory distress syndrome, chronic obstructive lung disease, and cystic fibrosis (28). Interestingly, we show here that oral delivery of either ManLAM, or the more potent 3T mannodendrimer, prevents lung inflammation by reducing neutrophil recruitment in mice exposed to aerosolized LPS. This antiinflammatory effect was found to be dependent on the murine DC-SIGN homolog SIGNR1. 3T antiinflammatory activity was further supported by histopathology analysis of the lung showing reduced alveolar wall thickening and inflammatory cell infiltration. Cytokine assay in the BALF revealed that 3T lowered TNF-α release but had no significant impact on IL-10, in contrast to in vitro data. The in vivo mechanism by which neutrophil recruitment is inhibited remains an open question but does not seem to involve CXCL-1 or CXCL-2 chemoattractants. It has been recently reported that oral delivery of BSA bearing mannosyl units induces oral tolerance in a model of food-induced anaphylaxis (29). Targeting SIGNR1 was proposed to help to condition DCs in the gastrointestinal lamina propria, promoting the generation of $CD4^+$ type 1 regulatory T-like cells that expressed IL-10 (29).

In conclusion, PPH dendrimer of third generation capped with trimannoside units (3T) is a type of fully synthetic powerful antiinflammatory molecule. Its mode of action is original and different from that of corticosteroids, which are classically used to fight inflammation, but are nonspecific, immunosuppressive, and can be deleterious during prolonged or high-dose therapy (30). These synthetic mannodendrimers, and more particularly 3T, should be tested in different pathologically models to determine the broader applicability of their therapeutic use.

Materials and Methods

Synthesis of PPH Dendrimers and Coupling of Oligomannosides. The synthesis of dendrimers was carried out as reported previously from a cyclotriphosphazene core (12). Each dendrimer was functionalized on the terminal

phosphorus atoms with *N*-BOC-tyramine. BOC deprotection gave the amino dendrimer, isolated as the trifluoroacetate salt as previously described (31). The oligomannosides, synthesized as described in *SI Materials and Methods* (13), were conjugated on the amino groups of the tyramine using the acyl azide method (14). More details are provided in *SI Materials and Methods*.

Inhibition Binding Assays. Binding inhibition assays were performed with (*i*) a soluble form of DC-SIGN fused to a 6 His-Tag (sDC-SIGN) (Fig. S3*A*) produced in *Escherichia coli* BL21 plysS and *Mycobacterium bovis* bacillus Calmette–Guérin ManLAM-coated microplates (100 ng per well) (Fig. S3*B*); and (*ii*) a membrane-expressed form of DC-SIGN (mDC-SIGN) using HEK transfectants stably expressing wild-type DC-SIGN tagged with GFP (HEK::DC-SIGN) (Fig. S3*C*) and *Saccharomyces cerevisae* mannan-coated microplates (10 μg per well) (Fig. S3*D*). More details are provided in *SI Materials and Methods*.

Cytokine Production by DCs. Human monocyte-derived DCs were generated as previously described (1). Immature DCs were incubated in RPMI 1640, 10% FCS (Lonza) with the indicated products and assessed for cytokine production after 18 h. *E. coli* K12 ultrapure LPS (Invivogen) was used at a concentration of 20 ng/mL, *M. bovis* bacillus Calmette–Guérin ManLAM (1) at 0.6 μM (10 μg/mL), and mannodendrimers at 0.3 or 0.6 μM. To investigate DC-SIGN dependence, DCs were preincubated for 30 min at 37 °C with 20 μg/mL anti–DC-SIGN (clone AZND1; Beckman Coulter) or isotype control antibodies. TNF-α, IL-6, IL-10, and IL-8 were assayed in the supernatant by sandwich ELISA using commercially available kits (eBioscience). Measurement of Raf-1 phosphorylation induced by 3T was performed as described by Gringhuis et al. (6) (*SI Materials and Methods*).

Neutrophil Recruitment and Cytokine Release in LPS-Aerosolized Mice. Adult female BALB/c and C57BL/6 mice (8–10 wk old) were obtained from Janvier. *Signr1*-deficient mice (19) were bred in the animal breeding facility of Institut de Pharmacologie et de Biologie Structurale. All mice were housed under specific pathogen-free conditions, had access to food and water ad libitum, and were treated according to the Institut National de la Recherche Agronomique and Centre National de la Recherche Scientifique guidelines for housing and care of laboratory animals. All protocols were reviewed and approved by the Regional Ethics Committee of Midi-Pyrénées (France) for Animal Experimentation (authorization no. MP/02/69/10/12). Mice received ManLAM or dendrimers solutions (1 mg/kg) daily for 15 d via a gavaging needle. Control animals were treated daily with sterile 0.9% NaCl alone. BALF was collected 18 h after *Pseudomonas aeruginosa* LPS (1 mg/mL) (S10; Sigma) or vehicle (saline: sterile 0.9% NaCl) nebulization (1 mL during 1 h) by cannulating the trachea under deep pentobarbital anesthesia and washing the lung twice with 1 mL of saline at room temperature. The total cell numbers were counted using a Coulter counter (Beckman). Smears of BALF cells were prepared using a Cytospin (Shandon) and stained with May–Grünwald stain for differential cell counts. A total of 200 cells were counted for each lavage and the absolute number of neutrophils was determined. An independent observer blinded to the experimental conditions performed all cell counts. Cytokines and chemokines were assayed in the BALF, collected 3 h after LPS challenge, by sandwich ELISA using commercially available kits (eBioscience; R&D Systems).

ACKNOWLEDGMENTS. We gratefully acknowledge Prof. Brigitte Gicquel (Institut Pasteur) for providing an *Escherichia coli* strain expressing recombinant sDC-SIGN, Dr. Kurt Drickamer (Imperial College) for Rat6::hMR and Rat6::SR1 transfectant cell lines, Dr. Olivier Neyrolles for the *Signr 1*$^{-/-}$ mice and Raw::SIGNR3 cells, and Dr. Pierre Lutz and Mr. Arnaud Métais for murine DCs. We also thank Dr. Mary Jackson for providing a critical reading of the manuscript. This work was supported by Centre National de la Recherche Scientifique and Université Paul Sabatier.

1. Nigou J, Zelle-Rieser C, Gilleron M, Thurnher M, Puzo G (2001) Mannosylated lipoarabinomannans inhibit IL-12 production by human dendritic cells: Evidence for a negative signal delivered through the mannose receptor. *J Immunol* 166(12):7477–7485.
2. Nigou J, et al. (2002) Mycobacterial lipoarabinomannans: Modulators of dendritic cell function and the apoptotic response. *Microbes Infect* 4(9):945–953.
3. Pitarque S, et al. (2008) The immunomodulatory lipoglycans, lipoarabinomannan and lipomannan, are exposed at the mycobacterial cell surface. *Tuberculosis (Edinb)* 88(6): 560–565.
4. Geijtenbeek TB, et al. (2003) Mycobacteria target DC-SIGN to suppress dendritic cell function. *J Exp Med* 197(1):7–17.
5. Maeda N, et al. (2003) The cell surface receptor DC-SIGN discriminates between Mycobacterium species through selective recognition of the mannose caps on lipoarabinomannan. *J Biol Chem* 278(8):5513–5516.
6. Gringhuis SI, et al. (2007) C-type lectin DC-SIGN modulates Toll-like receptor signaling via Raf-1 kinase-dependent acetylation of transcription factor NF-kappaB. *Immunity* 26(5):605–616.
7. Gilleron M, Jackson M, Nigou J, Puzo G (2008) Structure, biosynthesis, and activities of the phosphatidyl-myo-inositol-based lipoglycans. *The Mycobacterial Cell Envelope*, eds Daffe M, Reyrat J (ASM, Washington, DC), pp 75–105.
8. Rivière M, Moisand A, Lopez A, Puzo G (2004) Highly ordered supra-molecular organization of the mycobacterial lipoarabinomannans in solution. Evidence of a relationship between supra-molecular organization and biological activity. *J Mol Biol* 344(4):907–918.
9. Mitchell DA, Fadden AJ, Drickamer K (2001) A novel mechanism of carbohydrate recognition by the C-type lectins DC-SIGN and DC-SIGNR. Subunit organization and binding to multivalent ligands. *J Biol Chem* 276(31):28939–28945.
10. Feinberg H, Mitchell DA, Drickamer K, Weis WI (2001) Structural basis for selective recognition of oligosaccharides by DC-SIGN and DC-SIGNR. *Science* 294(5549):2163–2166.
11. Caminade AM, Turrin CO, Laurent R, Ouali A, Delavaut-Nicot B (2011) *Dendrimers: Towards Catalytic, Material and Biomedical Uses* (Wiley, Chichester, UK).
12. Launay N, Caminade A-M, Majoral J-P (1997) Synthesis of bowl-shaped dendrimers from generation 1 to generation 8. *J Organomet Chem* 529(1-2):51–58.
13. Peters T (1991) Synthesis and conformational analysis of methyl 2-*O*-(α-D-mannopyranosyl)-α-D-mannopyranoside. *Liebigs Ann Chem* (2):135–141.
14. Chatterjee D, et al. (1988) Synthesis and immunoreactivity of neoglycoproteins containing the trisaccharide unit of phenolic glycolipid I of Mycobacterium leprae. *Carbohydr Res* 183(2):241–260.
15. Venisse A, Fournié JJ, Puzo G (1995) Mannosylated lipoarabinomannan interacts with phagocytes. *Eur J Biochem* 231(2):440–447.
16. Schlesinger LS, Hull SR, Kaufman TM (1994) Binding of the terminal mannosyl units of lipoarabinomannan from a virulent strain of Mycobacterium tuberculosis to human macrophages. *J Immunol* 152(8):4070–4079.
17. Rolland O, et al. (2008) Tailored control and optimisation of the number of phosphonic acid termini on phosphorus-containing dendrimers for the ex-vivo activation of human monocytes. *Chemistry* 14(16):4836–4850.
18. Powlesland AS, et al. (2006) Widely divergent biochemical properties of the complete set of mouse DC-SIGN-related proteins. *J Biol Chem* 281(29):20440–20449.
19. Tanne A, et al. (2009) A murine DC-SIGN homologue contributes to early host defense against Mycobacterium tuberculosis. *J Exp Med* 206(10):2205–2220.
20. Grandjean C, Rommens C, Gras-Masse H, Melnyk O (2000) One-pot synthesis of antigen-bearing, lysine-based cluster mannosides using two orthogonal chemoselective ligation reactions. *Angew Chem Int Ed Engl* 39(6):1068–1072.
21. Pagé D, Roy R (1997) Synthesis and biological properties of mannosylated starburst poly(amidoamine) dendrimers. *Bioconjug Chem* 8(5):714–723.
22. Griffe L, et al. (2007) Multiplication of human natural killer cells by nanosized phosphonate-capped dendrimers. *Angew Chem Int Ed Engl* 46(14):2523–2526.
23. Garcia-Vallejo JJ, et al. (2013) Glycodendrimers prevent HIV transmission via DC-SIGN on dendritic cells. *Int Immunol* 25(4):221–233.
24. Cambi A, et al. (2004) Microdomains of the C-type lectin DC-SIGN are portals for virus entry into dendritic cells. *J Cell Biol* 164(1):145–155.
25. Tabarani G, et al. (2009) DC-SIGN neck domain is a pH-sensor controlling oligomerization: SAXS and hydrodynamic studies of extracellular domain. *J Biol Chem* 284(32): 21229–21240.
26. Shaunak S, et al. (2004) Polyvalent dendrimer glucosamine conjugates prevent scar tissue formation. *Nat Biotechnol* 22(8):977–984.
27. Andonegui G, et al. (2003) Endothelium-derived Toll-like receptor-4 is the key molecule in LPS-induced neutrophil sequestration into lungs. *J Clin Invest* 111(7): 1011–1020.
28. Zemans RL, Colgan SP, Downey GP (2009) Transepithelial migration of neutrophils: Mechanisms and implications for acute lung injury. *Am J Respir Cell Mol Biol* 40(5): 519–535.
29. Zhou Y, et al. (2010) Oral tolerance to food-induced systemic anaphylaxis mediated by the C-type lectin SIGNR1. *Nat Med* 16(10):1128–1133.
30. Barnes PJ (2011) Glucocorticosteroids: Current and future directions. *Br J Pharmacol* 163(1):29–43.
31. Rolland O, et al. (2009) Efficient synthesis of phosphorus-containing dendrimers capped with isosteric functions of amino-bismethylene phosphonic acids. *Tetrahedron Lett* 50(18):2078–2082.